IRAQI Academic Scientific Journals

Samarra Journal of Pure and Applied Science

SJPAS

www.sjpas.com

p ISSN: 2663-7405
e ISSN: 2789-6838

Using Treated Kenaf Plant Fibers as Absorbent Material to Remove Marine Oil Spill

Faieza S. Bodowara[1], Anad M. Alshaybani[2]
1- Department of Biomedical and Chemical Engineering and Sciences, Melbourne, USA.
2- Department of Chemistry, Faculty of Sciences, Sirte University, Libya

https://doi.org/10.54153/sjpas.2025.v7i1.841

Article Information

Received: 02/05/2024
Revised: 06/06/2024
Accepted: 10/07/2024
Published: 30/03/2025

Keywords:

Kenaf Plant, Oil Spill, Hydrophobicity, Optimization, Porosity, Retention Time, and Adsorption Capacity

Corresponding Author

E-mail:
aafhaima2011@my.fit.edu

Abstract

One of the most challenging problems related to modern industrial development is marine oil spills. Oil spills have significant detrimental effects on the marine environment and human life. The effects can be immediate through fish suffocation and erosion of their fins, deadly hypothermia in fur-bearing mammals, and ingestion when animals and birds try to clean up themselves. Oil spills also have long-term ecological effects, which lead to an interruption of the marine food chain. When oil reaches the coast, it interacts with beach sand and vegetation, causing damage to the human environment. These negative effects are exacerbated by changes in oil's physical and chemical properties after spilling. Many techniques have been invented to eliminate oil spills. However, almost all developed techniques cannot completely remove oil from the seawater. One of the most efficient oil cleanup techniques uses absorbing materials. Of particular interest are techniques that use natural organic (vegetative) materials. These materials possess many desirable characteristics: they are cheap, readily available, renewable, and biodegradable. However, to be competitive with the synthetic absorbers, the natural absorbers often require additional processing. A typical modification procedure includes carbonization, which increases surface hydrophobicity and improves oil-absorbing characteristics. Rational optimization of oil-absorbing properties requires quantitative characterization of the physic-chemical properties of absorbing materials during processing. However, current literature lacks such description-making material's modification as a trial-and-error procedure. In this document, I propose to develop an optimized modification procedure for a new absorbing material based on the carbonization of a widely available kenaf plant (*Hibiscus Cannabinus*). Quantitative optimization of the absorbing characteristics of kenaf fibers will be based on monitoring their physical and chemical changes during the carbonization process by using gas sorption analysers and IR-reflection spectroscopic techniques. A quantitative understanding of relevant parameters (for example, the relative abundance of surface polar and non-polar groups) will facilitate reproducibly optimal manufacturing.

Introduction and Related Work:

The dramatic growth of exploration, refining, and oil production is responsible for increased marine oil spills [1,2], which has become one of the most challenging chemical contamination problems and a serious global concern. Marine and wildlife become threatened by the immediate and long-term ecological effects of oil spills [3-5]. Furthermore, oil spills usually undergo various physical and chemical changes, such as spreading, photolysis, sedimentation, dissolution, and the formation of water-oil emulsions that can multiply the oil spill risks [6,7]. The effects of oil spills and the degree of danger that they present depend on the properties of the oil as well as on environmental parameters such as weather, sea state, and oil spill location [8,9]. For example, the spreading of oil spills over the sea depends on the viscosity and specific gravity of the oil, as well as the oil-water surface tension [10]. The lower the surface tension, the faster the spreading of oil over the sea, disregarding environmental factors such as wave height, current velocity, and wind speed. Further, the spreading of oil is accelerated in warmer water because of decreased surface tension and oil viscosity [11]. On the other hand, the high viscosity of an oil spill has another undesirable effect: it facilitates the formation of an oil-in-water emulsion (called "chocolate mousse") that has a grease-like consistency and is difficult to treat [12,13].

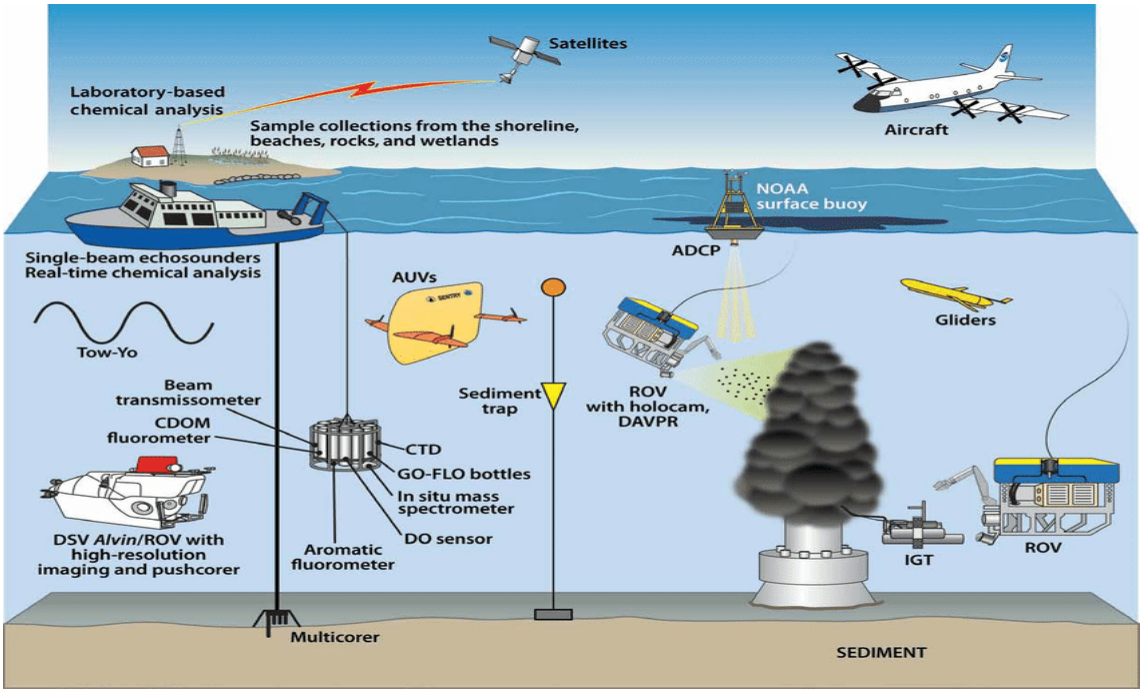

Fig. 1 *Methods of Oil Spill Clean-up [65].*

Additionally, the risk of the lighter components of oil that evaporate, especially in warm weather, cannot be disregarded. Evaporation increases the specific gravity of oil so that it may sink as tar balls and contaminate the seabed (sedimentation). The difficulties in solving the oil spill problem refer to the complex nature of oil; its components do not behave the same [14-16]. For this reason, the total elimination of oil is expensive (the average cost of cleaning a crude oil spill is $2730 per barrel [17], which exceeds the commercial oil price by a factor of approximately 50). Generally, we can classify the oil spill remediation techniques into physical, chemical, thermal, and biodegradation methods [18]. The physical methods include skimmers, booms, and adding absorbents [19]. Skimmers can be successfully used for

shorelines and calm seas, but they cannot deal with thick oil or floating debris because of their rigidity [20]. The more flexible type, boom, has certain successful applications and is also used in situ burning methods [21,22], but other issues still exist involving high cost, low efficiency, and being difficult to use, clean, or store [23], in addition to the high risk of in situ burning that threatens the marine environment [18,24,25]. The bioremediation method has relatively little cost and footprint [26]. Excellent remediation has been made by the bioremediation method in warm areas, such as in Mexican golf in 2010 [27]. In this method, microorganisms can degrade both aromatic and paraffinic hydrocarbons [18]. Yet, in many regions, several procedures are usually needed to simulate the proliferation of microbes, such as the injection of oxygen to motivate microbial activity [28]. Further, different strains of bacteria and fungi are needed to degrade all of the crude oil components, not just single species [28], in addition to the rarity of bacteria in very cold areas. Adding hydrophobic adsorbents is the most attractive method for finishing oil spill elimination [29-31]. Adsorbents are readily available and less expensive [32,33]. They can be used for all kinds of oil because of the wide variety of hydrophobic adsorbent materials [31]. The adsorption method is used as a final step in the oil spill cleanup because of its optimal effectiveness. Moreover, it can be used regardless of the weather and sea state. Absorbent materials have been classified into three types: organic polymers (synthetic), natural inorganic (mineral), and natural adsorbents. Polyurethane and polypropylene are the most common commercial sorbents [34,35]. Because these materials have high oleophilic and hydrophobic characteristics [36, 37], they can absorb oil several times their weight (polypropylene fibres have the highest oil absorption of 4.5 g of gasoline per gram of polypropylene) [34,38]. Yet, these materials are non-biodegradable [39]. Natural inorganic adsorbents such as silica, clay, and volcanic ash have lower costs and sorption capacities than those of synthetic materials [40-42]. However, their loose structures help them spread up, cause suffocation for labourers, and may damage the respiratory system after prolonged exposure [43]. To overcome the limitations of previous methods, vegetative fibers such as kapok and straw have considerable advantages related to their biodegradability, renewability, and high absorption capacity (the mass of absorbed oil is 3–15 times their weight) because of their hollow and fibrous structures [31,36-39]. Vegetative fibers have recently been modified to develop their absorption characteristics [44-47]. Though their preparation processes are relatively long and might decrease their biodegradability, Furthermore, the complexity of the steps makes the product unsuitable for reproducible manufacturing [36,48-54]. This study aims to introduce quantitative analyses, streamline the optimization process, and eliminate the need for redundant testing. Specifically, the project concentrates on formulating an optimized modification procedure for a novel absorbent material derived from the easily accessible Kenaf plant (Hibiscus cannabinus). In this study, Kenaf plant samples were subjected to varied temperatures during carbonization while employing in situ Attenuated Total Reflectance Fourier Transform Infrared Spectroscopy (ATR-FTIR) and gas sorption analysis to evaluate the resultant chemical and morphological alterations.

Research Methods (Material & Methods)

Proposed Framework

This study presents a method for optimizing Kenaf absorption characteristics. In this section, the theoretical formula has been applied for calculation.

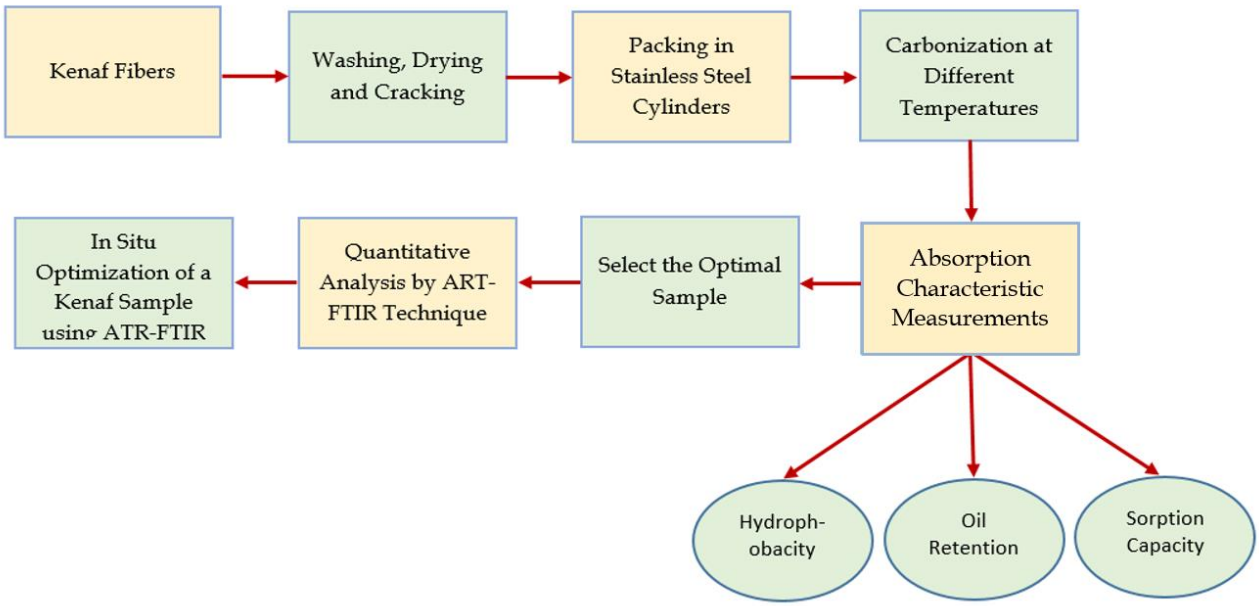

Fig. 2 *The proposed method for optimization of kenaf adsorption characteristics.*

The proposed methodology for kenaf is described in many stages that will be used in this experiment as summarized in Fig. 2 as follows:

Sample Preparation

The fresh Kenaf plant was washed with water to remove soil, inorganic, and foreign materials, dried for a week under the sun, and then dried at 105 ˚C for 2h in atmospheric air [55,56].

Carbonization of kenaf samples at different temperatures

The carbonization process, as shown in Fig. 3, was carried out in a vacuum (500 Pa) at different temperatures (200 ˚C, 300 ˚C, 400 ˚C, 500 ˚C, and 600 ˚C). The temperature rate increased by 5 ˚C, and each temperature was maintained for 1 h. Then, Kenaf was crushed into particles with ~ 200–900 µm diameter.

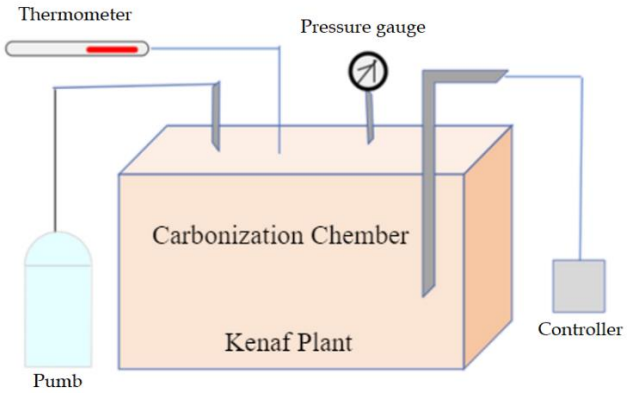

Fig. 3 *Describes the carbonization process of Kenaf controlled by required instruments*.

Measurements of absorption properties:

The absorption properties of carbonized samples at each temperature were measured using one of the most common oil derivatives, diesel. A mesh stainless steel test cell with a 17.5 cm^2 cross-section area and 10 cm long was packed with crushed Kenaf to produce a packing density of 0.03 g/cm^3, which was found to be a suitable packing density of vegetative sorbent for oil remediation [57]. Then, the test cell was dropped into the bath of diesel and seawater for specific times of 500–1000 s (the expected times for reaching the equilibrium of oil absorption). The oil-saturated test cells were taken from the baths and left for 1 minute to drain the free oil from the test cells [57]. The amount of oil that remained in Kenaf samples at each equilibrium time was measured and used for calculating oil absorption capacity by Eq. 1.

$$q_t = \frac{V_{C_0} - C_t}{w} \qquad (1)$$

where q_t (mg/g) is the amount of absorption at the equilibrium time t, C_0 and C_t are the concentrations of oil (mg/l) at the initial and equilibrium times, V is the water volume (l), and W is the dry mass of the absorbent (g) [58].

Oil retention

It is important to evaluate the ability of Kenaf to retain the absorbed oil during transfer and handling operations. At the end of the respective soaking time (at equilibrium), the oil-saturated cell was lifted above the oil bath for 60 min, allowing free oil to drop out of the cell. The weight of the cell was continuously recorded during that time. Then, the oil retention was calculated as follows:

$$Oil\ Retention = \frac{S_T - S_C - S_A}{S_A} \qquad (2)$$

where S_T is the total weight of oil, cell, and kenaf, S_C is the weight of the cell, and S_A is the dry weight of Kenaf.

Spontaneous imbibition phenomena

Figure 4 describes a theoretical model for spontaneous imbibition in porous media, which has previously been discussed by Li G. 2015 [59], Yu B. 2008 [60], Liu Y. 2007 [61], and Cai J. 2010 [62].

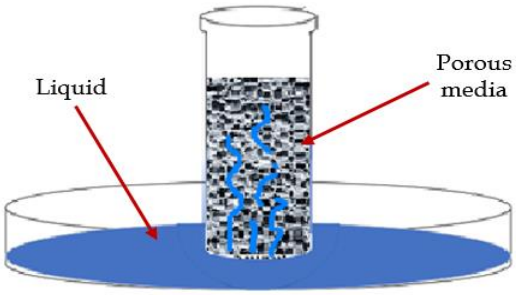

Fig. 4 *Schematic of spontaneous imbibition phenomena.*

The model was used to describe the absorption process of oil through the carbonated Kenaf plant. The weight of imbibed oil increases with time, according to eq. 3:

$$W^2 = (Af\varphi\rho)^2 \frac{R_{eff}\gamma cos\theta}{2\eta} \qquad (3)$$

where W denotes the weight of oil, ρ is the density of oil (Diesel = 0.38 g/cm^3), A_f stands for cross-section areas of the sample (A_f = 17.5 cm2), which could be measured using the SEM technique, φ is the porosity of carbonated kenaf sample, which can be determined using a gas sorption analyzer, γ is the surface tension of oil (for diesel = 26.29 mN m^{-1}), θ is the contact angle between oil and sample surface, η is the viscosity of oil (for diesel= 5 mN.sm^{-2}), t is the imbibed time, and R_{eff} is the effective capillary radius, which can be calculated as follows:

$$R_{eff} = \frac{1}{2\tau_a^2}\frac{2-D_f}{3-D_f}\frac{\lambda_{max}}{1-\varphi} \qquad (4)$$

where τ_a is the tortuosity of the streamlines in the porous media ($\tau_a = 1 + 0.41\, ln\frac{1}{\varphi}$), D_f is the pore fractal dimension, λ_{max} is the maximum pore diameter. D_f can be obtained from the following equation:

$$D_f = d - \frac{ln\varphi}{ln\xi} \qquad (5)$$

where d is the Euclidean dimension (consider d = 2), and ξ is considered a coefficient of friction per unit length of the wetting line (consider ξ = 0.01 Pa.s). The maximum pore diameter, λmax, can be calculated from the Cai J. expression.

$$\lambda_{max} = \frac{D_s}{4}\left[\sqrt{\frac{2\varphi}{1-\varphi}} + \sqrt{\frac{\varphi}{1-\varphi}} + \sqrt{\frac{\pi}{1-\varphi}} - 1\right] \qquad (6)$$

Ds is characteristic particle diameter (Consider *Ds* = 200 μm).

Results and Discussions

Results of the Experiment

By solving equation 1, the weight of imbibed oil was obtained at the given times. Figure 5 shows the weight of oil absorbed during the imbibition process of our sample. A similar relationship has been obtained in previous research on the kenaf plant using the same equation [59]. Indicating the spontaneous manner of oil spill elimination.

It's observed that the amount of absorbed oil at equilibrium does not depend on the imbibition time, which can also be seen in the previous work. When the kenaf sample attains optimal absorption capacity, the absorbed oil can reach a much larger weight than the sample.

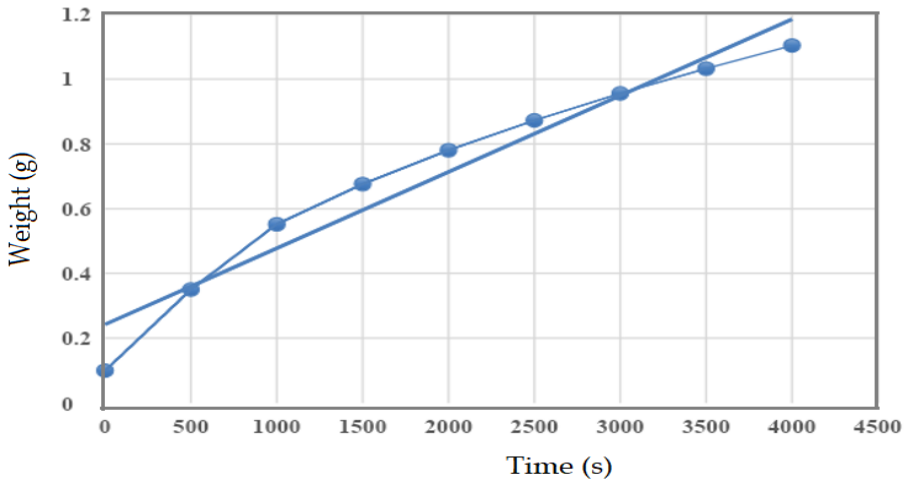

Fig. 5 *Theoretical Model for Spontaneous Imbibition in Porous Media on the Proposed Data.*

By increasing the carbonization temperatures of Kenaf fibers, the porosity was promoted, hence the absorption capacity of oil. However, the improperly high carbonization temperature leads to the collapse of the lumen and creates large inter-fiber pore spaces, which are unsuitable for absorbing low-density petrol derivatives. Therefore, an evaluation of the absorption process is needed at each temperature to find the optimal characteristics. Figure 6 shows the experimental results of the oil retention for Kabok assemblies with different loose structures [57]. The higher the packing structure, the greater the amount of oil retention, whereas the lowest packing structure quickly dripped oil from the assemblies. This is because of the large inter-fibers distance and, consequently, the destabilization of the oil bridges that form between fibers [63]. The same experiment can be performed to optimize the absorption characteristics of Kenaf, and a similar result is expected since both Kenaf and Kabok have similar lignocellulose structures [64]. Increasing the carbonization temperature leads to an increase in the porosity of fibers, which is recommended for extending the absorption capacity. However, as shown in Fig. 6, the extremely loose fibers will allow higher percentages of oil to drip out quickly during transfer operations. Therefore, a compromise should be considered to reach satisfactory values of absorption capacity and oil retention percentage.

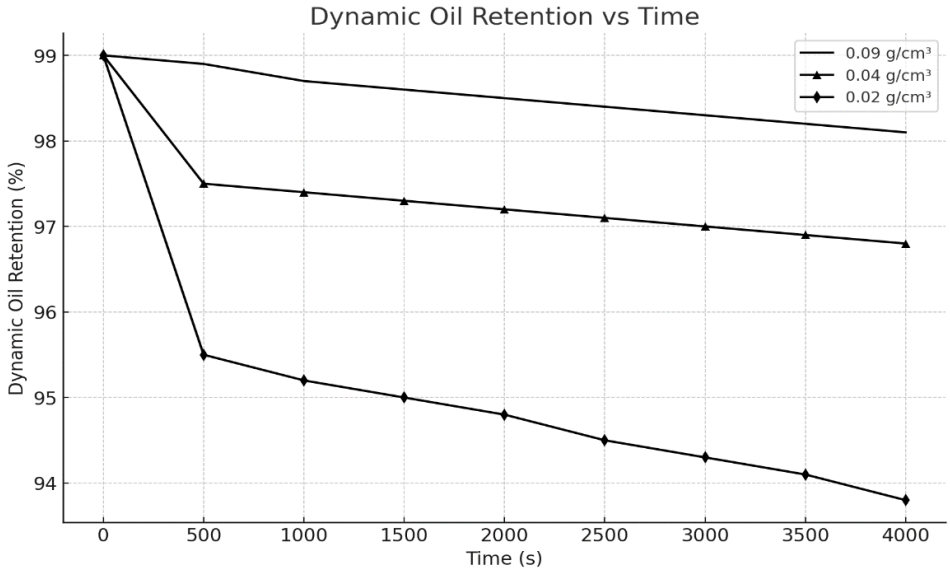

Fig. 6 *Shows oil retention controlled by the porosity of the absorbent.*

Evaluation of hydrophobicity

Most natural fibers have a waxy inside surface, which increases the selectivity of hydrophobic liquids over water [57]. For example, Kabok fibers show excellent hydrophobicity compared to polypropylene and, hence, high selectivity for oils with different densities [57]. Particularly, the lighter oil, diesel, could be fully removed from the water.

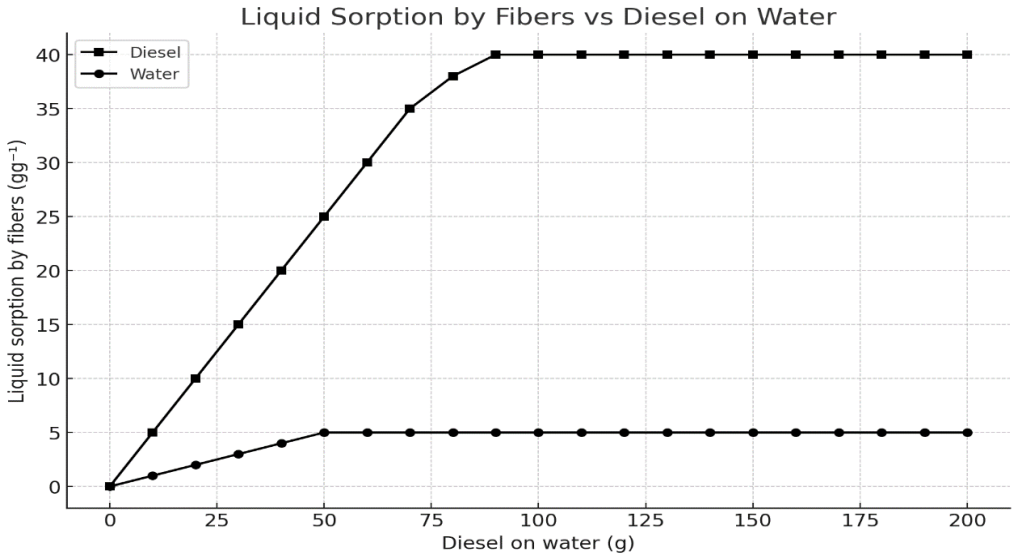

Fig. 7 *Shows an optimal selectivity of Kabok fibers for diesel oil from water [52].*

This is expected since diesel is a relatively light oil and could enter the fibers easily. The reason for the inability of water to penetrate this fiber might be due to the presence of negative capillary entry pressure resulting from the large contact angle (> 90°) and surface tension of water against the air in the pores [65]. The same experiment was performed in this research, and Fig. 7 is considered a benchmark for optimal hydrophobic conditions.

The reproducible quantitative analysis of an optimized Kenaf sample

After recognizing the temperature at which the optimal absorption characteristics are attained, the carbonized Kenaf at the favorable temperature (optimized sample) will undergo quantitative analyses by using the ATR FTIR technique to determine the main components of this sample. The optimization process was carried out simply by carbonizing a kenaf sample at the desired temperature and optimizing it *in situ by* determining the chemical changes of the sample using the FT-IR technique in ATR mode [66].

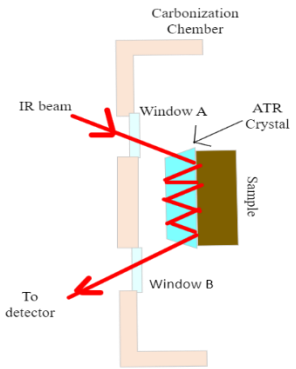

Fig. 8 *Modification for in situ monitoring of the chemical transformation of absorbent material during the carbonization process.*

Figure 8 is proposed to illustrate a scheme for monitoring the functional group changes of the sample during carbonization. An ATR accessory with a 45C° Zinc selenide, ZnSe crystal flat plate was coupled with a spectrometer for data acquisition. The crystal was placed into the carbonization chamber and in intimate contact with the sample by using a built-in pressure applicator [53]. The spectrometer was first purified by a pure gas generator and an oil-less air compressor before sample analysis [67]. Before the calibration, it is necessary to know the functional groups to be determined. Cellulose molecules consist mainly of repeating glucose units; therefore, the functional groups that represent cellulose are mainly hydroxyl groups, three of which are linked to each glucopyranose unit. The whole structure of cellulose is constructed by hydrogen bonds that connect cellulose chains [68]. Levoglucosan compound, which contains a ketal functional group, was formed by carbonization (Fig. 9) and increased until the temperature reached 580°C, then started to decrease with elevating temperature.

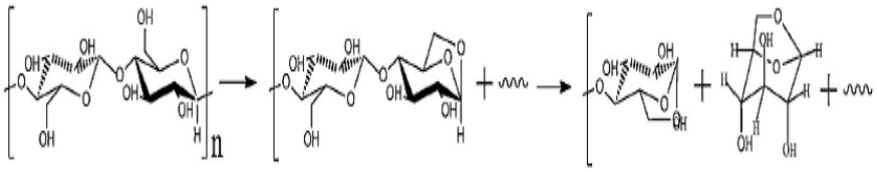

Fig. 9 *Formation of Levoglucosan in the early stages of cellulose carbonization [70].*

On the other hand, the other competitive compound, hydroxy acetaldehyde which will also be formed from cellulose carbonization will increase steadily with temperature [68]. The other main part of the kenaf structure is the polyaromatic lignin compound, which, after carbonization, gives low molecular weight aromatic compounds with phenolic units [68]. Therefore, monitoring the chemical transformation of kenaf samples requires a range of ATR spectrums that include the bands of carbohydrate hydroxyl, C-OH stretch (3500-2600 cm^{-1}) [69], ketal, R – O – C – O–R stretch (1381- 1217 cm^{-1}) [65], and aldehyde, R–C(O)H stretch (1700 cm^{-1}) [53] functional groups. Monitoring lignin decomposition might not be clear because the aromatic functional group concentration will not be changed after lignin depolymerization. Therefore, by increasing the ketal of levoglucosan or aldehydes groups and decreasing the hydroxyl of polysaccharide the chemical changes of the kenaf sample can be determined.

The calibration was carried out by entering the same functional groups with known molar concentrations, excluding outlier bands that can cause substantial errors, and then the calibration was selected after two different normalization procedures [53]. To quantify the chemical changes during carbonization, it is useful to obtain the ATR spectra of the same species before starting this process. Then, the spectra during the carbonization were compared with those for the untreated sample [53]. The measurements were performed by choosing a wave number range of 4000-500 cm^{-1}, spectral resolution of 4 cm^{-1}, and 40 scans per sample. By using the same parameters, a spectrum without any material on the diamond crystal was obtained. This void spectrum is considered a background and is needed before each sample measurement. Then, ATR spectra were also compared to those obtained in Section 3 (at the same operational parameters) for the sample at the same optimum temperature, and the two measurements are expected to be similar.

Statistical Analysis

In this section, we employed modeling and optimization techniques to establish correlations between independent variables, including retention time in seconds (X1), particle size in micrometers (X2), and packing density in g/cm^3 (X3), and their impact on the predicted oil retention percentage (Y). The findings from these investigations, which encompassed 10 experimental runs, are summarized in Table 1. This table provides a comprehensive view of the Response Surface Methodology (RSM) model, illustrating the relationships between these variables and their respective experimental and predicted oil retention.

Table 1: Model of Response Surface Methodology

Run #	Temp. (C°)	Retention time (s) (X_1)	Particle size (µm) (X_2)	Packing density (g/cm^3) (X_3)	Experimental oil retention (Y)	Predicted oil retention %
1	100	500	50	0.10	10.1	10.3
2	200	1000	150	0.09	17.3	19.2
3	300	1500	250	0.08	30.5	32.7
4	400	2000	350	0.07	37.5	40.6
5	500	2500	450	0.06	51.6	55.4
6	600	3000	550	0.05	76.3	79.5
7	700	3500	650	0.04	81.6	84.2
8	800	4000	750	0.03	85.1	86.3
9	900	4500	850	0.02	85.4	86.3
10	1000	5000	950	0.01	85.5	86.4

In this analysis, we have interpreted the correlations derived from the provided dataset and delved into their implications, as illustrated in Fig. 10. The correlation heatmap visually represents the strength of linear relationships between pairs of features, specifically retention time in seconds, particle size in micrometers, and packing density in g/cm^3. A positive correlation is evident between retention time and particle size, indicating that as particle size increases, there is a corresponding increase in retention time.

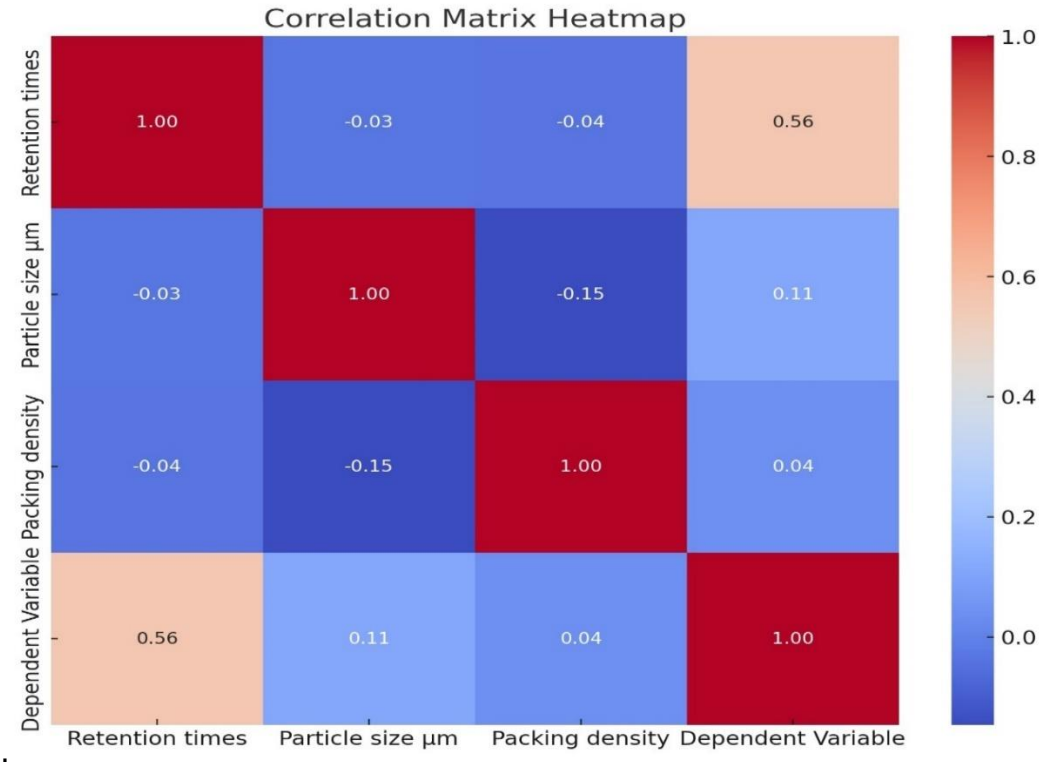

Fig.10 *Correlation heatmap*

As a result, we noted a positive correlation between retention time and packing density. This relationship suggests that the larger the packing density, the longer the retention time tends to be. This correlation can be attributed to the fact that denser packing causes greater resistance, leading to a slowdown of particle flow and, as a result, longer retention times. These notes shed light on the dynamic interaction of these variables in the oil retention process. There is a direct correlation between experimental oil retention and both retention time and particle size. Contrariwise, there exists an opposite correlation between experimental oil retention and packing density, as illustrated in Fig. 11. These observations emphasize the substantial effect of these variables on both the oil retention process and underline the significance of the impact of these relationships.

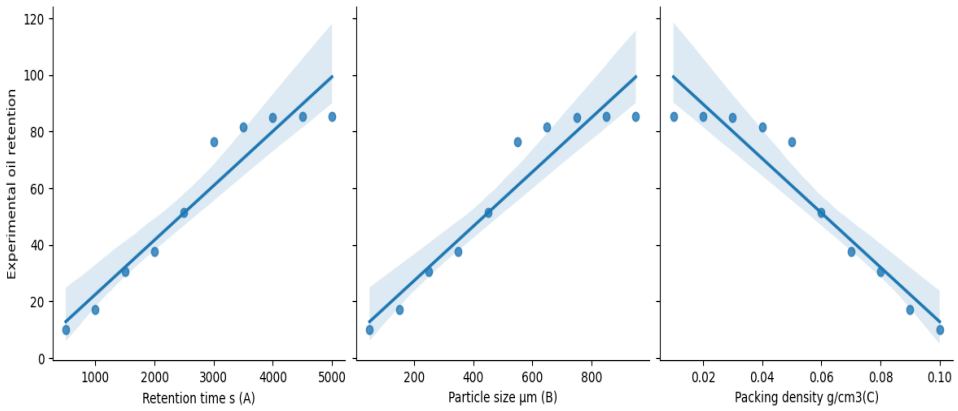

Fig. 11 *Relationship between experimental oil retention and Retention time, Packing density, and Particle size.*

Table 2 displays and Fig 12 comprehensive overview of our linear regression model, providing vital insights into its coefficients, R-squared (R-sq) value, adjusted R-squared (R-sq(adj)) value, and mean squared error (MSE).

Table 2: Linear Regression model

Term	Feather	Coef	R-sq	R-sq(adj)
b 0	Constant	4.89		
b 1	Retention times	$1.8372e^{-02}$	97.83%	97.86%
b 2	Particle size (µm)	$3.67544e^{-03}$		
b 3	Packing density	$-3.67e^{-07}$		

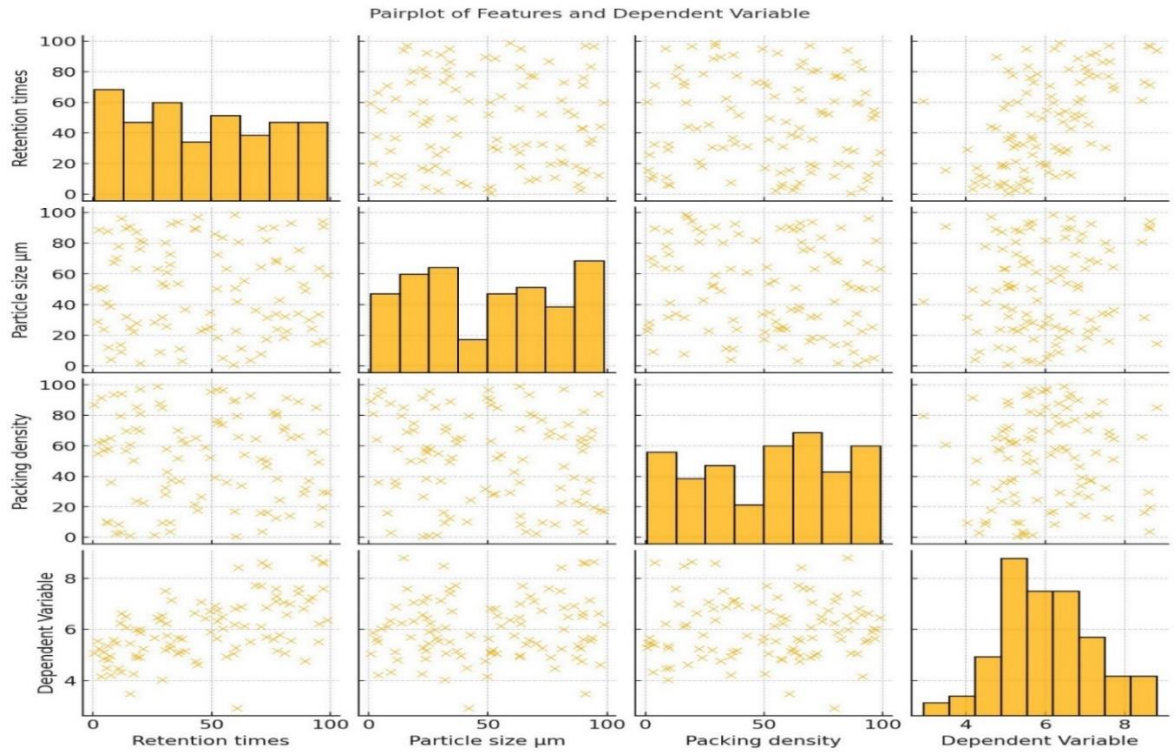

Fig.12 *Pair plot of feathers and Dependent Variables*

Predictive Model (Equation 1): The predictive model for the oil retention percentage (predicted oil retention %) is presented in Equation 7:

$$\text{Predicted oil retention \%} = 4.89 + 1.8*e^{-02} X_1 + 3.6*e^{-03} X_2 - 3.6*e^{07} X_3 \quad (7)$$

where X_1 is Retention times, X_2 is Particle size (µm), and X_3 is Packing density. The equation depicts the intricate relationship between the independent variables Retention Time, Particle Size, and Packing Density, and the dependent variable, Predicted Oil Retention. The intercept (b0) value in this equation is 4.89, which indicates the estimated oil retention percentage when all the independent variables (retention time, particle size, and packing density) assume a zero value. However,

experimentally, these variables rarely reach an absolute zero value, making interpreting this value somewhat abstract. The coefficient for retention time (b1), set at 1.8e-02, demonstrates that as the retention time in seconds increases, there is a corresponding increase in the predicted oil retention percentage. This suggests a positive relationship, where longer retention times result in higher oil retention, reflecting the effect of time in this process.

Moving on to particle size (b2), it stands at 3.6e-03, implying that an increase in particle size measured in micrometers is associated with a heightened predicted oil retention percentage. A positive relationship unfolds here, indicating that larger particles are more efficient at retaining oil in this context. In contrast, packing density (b3) is represented by -3.6e-07, revealing that higher packing density, expressed in g/cm^3, is tied to a modest reduction in predicted oil retention percentage. This signifies a negative relationship where denser packing conditions result in slightly decreased oil retention, likely due to increased resistance and slowed particle flow within the system. These coefficients offer critical insights into the strength and direction of the relationships between the independent variables and the predicted oil retention percentage, aiding in a better understanding of the dynamics at play in this complex system.

The R-squared value of 97.83% implies that the model explains a very high proportion of the difference in the dependent variable. This proposes that the model fits the data remarkably well. The adjusted R-squared value of 97.86% further confirms the goodness of fit, accounting for the number of predictors in the model. Both values highlight the effectiveness of the model in capturing the variability of the dependent variable based on the predictors used. Therefore, to analyze the relationship between experimental and predicted oil retention, we can see Fig. 13, where the results for both align almost closely. Our model is highly precise in its predictions, as the observed data closely reflect the values predicted by the model. This validation points out the robustness and reliability of our predictive model in real-world scenarios.

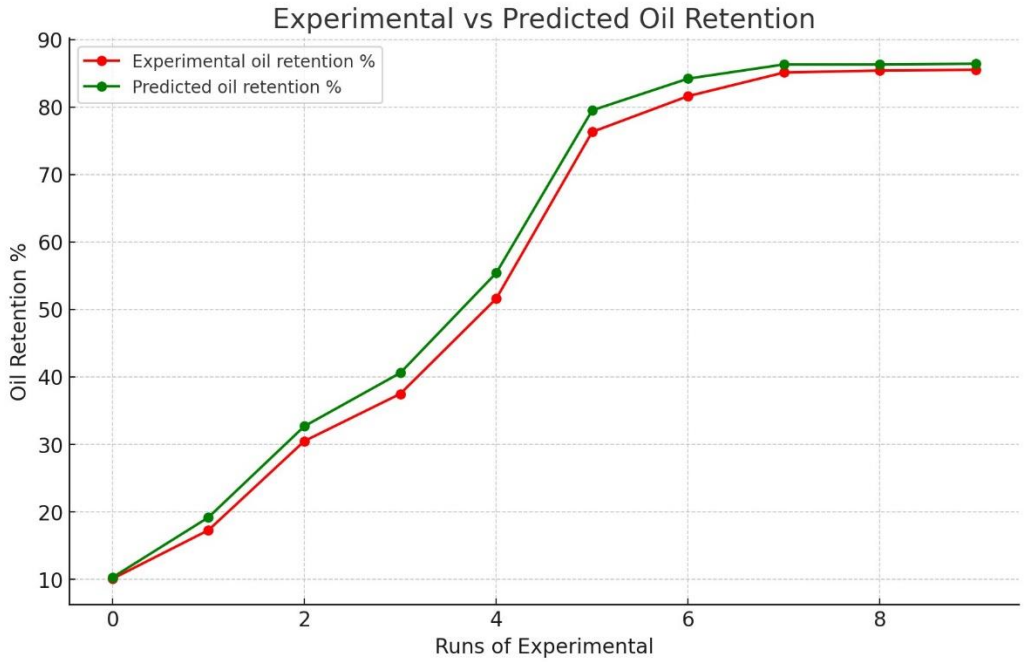

Fig 13. *Comparison between Experimental and Predicted Oil Retention.*

This study gives insight into a comprehensive understanding of Kenaf's physical-chemical properties, specifically focusing on variables such as retention time, particle size, packing density, and their effect on oil retention. By applying statistical modelling and quantitative analysis, we aim to create predictive models that will inform future experiments, optimizing Kenaf-based absorbents for oil spill removal. The research it tries to find is not only a significant contribution to the environmental remediation area but also aligns with the widely global purposes of sustainability and responsible resource management. Investigating the potential of Kenaf as a natural and eco-friendly oil absorbent would be a first step towards addressing a critical environmental challenge of our time.

First, it is necessary to conduct practical experiments to validate the predictive capabilities of the proposed model in real-world oil spill removal scenarios. This includes designing experiments that are performed according to the optimized physical-chemical parameters derived from this study. Furthermore, the environmental impact and cost-effectiveness of Kenaf-based absorbents in oil spill removal operations require in-depth investigation. Comparing the absorption capacity and cost-efficiency of Kenaf-based materials against traditional synthetic alternatives will provide useful and worthy data for decision-makers. Additionally, research should continue optimizing Kenaf-based absorbents' manufacturing process to achieve scalability and cost-effectiveness while maintaining high performance.

Conclusion

The extensive analyses undertaken in this study aimed to pinpoint the precise physical-chemical parameters necessary for the development of highly efficient Kenaf-based absorbents for marine oil spill cleanup. Kenaf's adaptability to various climates and its minimal labour-intensive cultivation process make it a promising candidate for widespread adoption in oil spill remediation endeavours. The statistical analysis, focusing on linear

regression, has unveiled intricate relationships among retention time, particle size, and packing density, providing valuable insights into their combined impact on oil retention percentages. Conspicuously, a substantial 97.86% of the total variation in oil retention percentage can be attributed to these variables under scrutiny. These statistical models offer a predictive framework for designing future oil retention experiments. By applying statistical predictions alongside rigorous quantitative analyses, we can streamline our path toward achieving oil spill cleanup objectives efficiently and in an environmentally sustainable manner. Kenaf's potential as a natural absorbent stands poised to make a significant and positive impact on the environmental remediation landscape.

Information on Author affiliations:
Faieza S. Bodowara[1], Anad M. A. Alshaybani [2]
1- Department of Biomedical and Chemical Engineering and Sciences, Melbourne, USA·
2- Department of Chemistry, Faculty of Sciences, Sirte University, Libya (**corresponding author**) (E-mail: aafhaima2011@my.fit.edu)

References

1. Annunciado, T. R., Sydenstricker, T. H., & Amico, S. C. (2005). Experimental investigation of various vegetable fibers as sorbent materials for oil spills. *Marine pollution bulletin*, *50*(11), 1340–1346. doi.org/10.1016/j.marpolbul.

2. Sun, Q., Liu, W., Wen, C., & Cai, L. (2024). Estimation of Marine Oil Spill Surface Characteristics Based on Laser-Induced Fluorescence with IA-DBSCAN. *IEEE Transactions on Instrumentation and Measurement, Instrumentation and Measurement, IEEE Transactions on, IEEE Trans. Instrum. Meas*, *73*, 1–14. https://doi-org.portal.lib.fit.edu/10.1109/TIM.2024.3396852.

3. Barron, M. G., Vivian, D. N., Heintz, R. A., & Yim, U. H. (2020). Long-Term Ecological Impacts from Oil Spills: Comparison of *Exxon Valdez*, *Hebei Spirit*, and Deepwater Horizon. *Environmental science & technology*, *54*(11), 6456–6467. https://doi.org/10.1021/acs.est.9b05020.

4. Chang, S. E., Stone, J., Demes, K., & Piscitelli, M. (2014). Consequences of oil spills: a review and framework for informing planning. *Ecology and Society*, *19*(2). doi.jstor.org/stable/26269587.

5. Soares, M. O., & Rabelo, E. F. (2023). Severe ecological impacts caused by one of the worst orphan oil spills worldwide. *Marine Environmental Research*, *187*. https://doi-org.portal.lib.fit.edu/10.1016/j.marenvres.2023.105936.

6. Adofo, Y. K., Nyankson, E., & Agyei-Tuffour, B. (2022). Dispersants as an oil spill clean-up technique in the marine environment: A review. *Heliyon*, *8*(8), e10153. https://doi.org/10.1016/j.heliyon.2022.e10153.

7. Ozhan, K. (2023). How weathering might intensify the toxicity of spilled crude oil in marine environments. Environmental Science and Pollution Research, 30(44), 99561–99569. https://doi-org.portal.lib.fit.edu/10.1007/s11356-023-29368-x.

8. Brannvall, E., (2008). Marine pollution: an overview, *Geochemistry 1*, 17-23. doi: 10.2478/v10056-008-0002-9.

9. Alonso-Alvarez, C., Pérez, C., & Velando, A. (2007). Effects of acute exposure to heavy fuel oil from the Prestige spill on a seabird. *Aquatic toxicology (Amsterdam, Netherlands)*, *84*(1), 103–110. doi.org/10.1016/j.aquatox.2007.06.004.

10. Li, C., Wang, Y., Zheng, L., Wang, J., Wei, S., & Yang, R. (2024). Spreading process and characteristics of silicone oil with multi-viscosities on calm liquid surface with low temperature: Spreading length, stable thickness and morphology. *Geoenergy Science and Engineering*, *233*. https://doi-org.portal.lib.fit.edu/10.1016/j.geoen.2023.212568.

11. Ivshina, I. B., Kuyukina, M. S., Krivoruchko, A. V., Elkin, A. A., Makarov, S. O., Cunningham, C. J., Peshkur, T. A., Atlas, R. M., & Philp, J. C. (2015). Oil spill problems and sustainable response strategies through new technologies. *Environmental Science: Processes & Impacts*, 17(7), 1201-1219. https://doi.org/10.1039/c5em00070j

12. Medeiros, A. D. L. M. D., Silva Junior, C. J. G. D., Amorim, J. D. P. D., Durval, I. J. B., Costa, A. F. D. S., & Sarubbo, L. A. (2022). Oily wastewater treatment: methods, challenges, and trends. *Processes*, *10*(4), 743.

13. Yan, K., Zhao, F., Pan, L., Jiang, Y., Shi, Y., & Yu, G. (2023). High-throughput clean-up of viscous oil spills enabled by a gel-coated mesh filter. *Nature Sustainability*, 6(12), 1654-1662. https://doi.org/10.1038/s41893-023-01217-2.

14. Mager, E. M., & Pasparakis, C. (2024). Crude oil-induced cardiotoxicity in fishes. *Encyclopedia of Fish Physiology*, 721-754. https://doi.org/10.1016/b978-0-323-90801-6.00077-x.

15. Harrison, R. M. (1996). Pollution Causes, Effects and Control. *Royal Society of Chemistry*: UK.

16. Schwarzenbach, R. P., Geschwind, P. M. Imbden, D. M., (1993). Environmental Organic Chemistry. *Wiley: New York*.

17. Davis, D.W.; Guidry, J. R. (1996). Oil spills and the state responsibilities, *Basin Res.*, 6, 60-68.

18. Dave, D., & Ghaly, A.E. (2011). Remediation Technologies for Marine Oil Spills: A Critical Review and Comparative Analysis. *American Journal of Environmental Sciences, 7*, 423-440.

19. Bhagwat, S. B., Jaspal, D., Tiwari, A. K., Malviya, A., & Petrounias, P. (2024). Sustainable polyurethane for the remediation of oil spills: a review. *Environmental Science and Pollution Research*, *31*(19), 27509–27530. https://doi-org.portal.lib.fit.edu/10.1007/s11356-024-33037-y.

20. Ventikos, N. P., Vergetis, E., Psaraftis, H. N., & Triantafyllou, G. (2004). A high-level synthesis of oil spill response equipment and countermeasures. *Journal of hazardous materials*, *107*(1-2), 51–58. doi.org/10.1016/j.jhazmat.

21. Hussein, M.H., Amer, A.A., & Sawsan, I.I. (2009). Oil Spill Sorption Using Carbonized PITH Bagasse. Application of Carbonized PITH Bagasse as Loose Fiber, *Global Nest Journal, 11*, 440-448. doi:10.30955/gnj.000539.

22. Schaum, J., Cohen, M., Perry, S., Artz, R., Draxler, R., Frithsen, J. B., Heist, D., Lorber, M., & Phillips, L. (2010). Screening level assessment of risks due to dioxin emissions from burning oil from the BP Deepwater Horizon Gulf of Mexico spill. *Environmental science & technology*, *44*(24), 9383–9389. doi.org/10.1021/es103559w.

23. Shilin, L., Lin, J., Chen, Q., Liu, Z., Gui, L., Chen, L., Huang, S., & Tian, X. (2021). A Strategy of Liquid-Grafted Slippery Sponges with Simultaneously Enhanced Absorption and Desorption Performances for Crude Oil Spill Remediation. *Macromolecular Materials and Engineering*.

24. Azevedo, A., Oliveira, A., Fortunato, A. B., Zhang, J., & Baptista, A. M. (2014). A cross-scale numerical modeling system for management support of oil spill accidents. *Marine pollution bulletin*, *80*(1-2), 132–147. doi.org/10.1016/j.marpolbul.2014.01.028.

25. Fingas, M. (1995). Oil Spills and Their Cleanup. *Chemistry & Industry*, 1005-1008.

26. Tyagi, M., da Fonseca, M. M., & de Carvalho, C. C. (2011). Bioaugmentation and biostimulation strategies to improve the effectiveness of bioremediation processes. *Biodegradation*, *22*(2), 231–241. doi.org/10.1007/s10532-010-9394-4.

27. https://www.mmc.gov/priority-topics/offshore-energy-development-and marine-mammals/gulf-of-mexico-deepwater-horizon-oil-spill-and-marine-mammals/.

28. Lim, M. W., Lau, E. V., & Poh, P. E. (2016). A comprehensive guide of remediation technologies for oil contaminated soil - Present works and future directions. *Marine pollution bulletin*, *109*(1), 14–45. doi.org/10.1016/j.marpolbul.2016.04.023.

29. Adebajo, M.O., Frost, R.L., Kloprogge, J.T., Carmody, O., & Kokot, S. (2003). Porous Materials for Oil Spill Cleanup: A Review of Synthesis and Absorbing Properties. *Journal of Porous Materials, 10*, 159-170.

30. OSS, Oil spill solution. Retrieved on 26th February, 2010 from http://www.oilspillsolutions.org/booms.htm.

31. Sabir, S.M. (2015). Approach of Cost-Effective Adsorbents for Oil Removal from Oily Water. Critical Reviews in Environmental Science and Technology, 45, 1916 - 1945.

32. Okiel, K., El-Sayed, M., & Elkady, M.Y. (2011). Treatment of oil–water emulsions by adsorption onto activated carbon, bentonite and deposited carbon. *Egyptian Journal of Petroleum, 20*, 9-15.

33. Muhammad, I.M., El-Nafaty, U.A., Abdulsalam, S., & Makarfi, Y.I. (2012). Removal of Oil from Oil Produced Water Using Eggshell. *Civil and environmental research, 2*, 52-63.

34. Mohammad, A. F., Mourad, A. A.-H. I., Galiwango, E., Lwisa, E. G., Al-Marzouqi, A. H., El-Naas, M. H., Van der Bruggen, B., & Al-Marzouqi, M. H. (2021). Effective and sustainable adsorbent materials for oil spill cleanup based on a multistage desalination process. *Journal of Environmental Management*, *299*. https://doi-org.portal.lib.fit.edu/10.1016/j.jenvman.2021.113652.

35. Jarre, W., Marx, M., Wurm,R. (1979). Polyurethanschaume mit hohem Olabsorp tionsvermogen. Die Angewandte Macromolecular, *Chemie*, 78, 67-74.

36. Banerjee, S. S., Joshi, M. V., & Jayaram, R. V. (2006). Treatment of oil spill by sorption technique using fatty acid grafted sawdust. *Chemosphere*, *64*(6), 1026–1031. doi.org/10.1016/j.chemosphere.

37. Karakasi, O.K., & Moutsatsou, A. (2010). Surface modification of high calcium fly ash for its application in oil spill cleanup. *Fuel, 89*, 3966-3970.

38. Ghaly, R.A., Pyke, J.B., Ghaly, A.E., & Ugursal, V.I. (1999). Remediation of diesel-oil-contaminated soil using peat. *Energy Sources, 21*, 785-799.

39. Choi, H., & Cloud, R.M. (1992). Natural sorbents in oil spill cleanup. *Environmental Science & Technology, 26*, 772-776.

40. Holakoo, L. (2001). On the capability of rhamnolipids for oil spill control of surface water.

41. Ding, Z., Kloprogge, J.T., Frost, R.L., Lu, G.Q., & Zhu, H.Y. (2001). Porous Clays and Pillared Clays-Based Catalysts. Part 2: A Review of the Catalytic and Molecular Sieve Applications. *Journal of Porous Materials, 8*, 273-293.

42. Alther, G.R. (2002). Removing oils FROM WATER with organoclays. *Journal - American Water Works Association, 94*.

43. USEPA, Sorbents. Emergency management. Retrieved on 7th March from http://www. epa. gov/OEM /content / learning /sorbent s.htm. 2011a.

44. Doshi, B., Repo, E., Heiskanen, J., Sirviö, J.A., & Sillanpää, M. (2018). Sodium salt of oleoyl carboxymethyl chitosan: A sustainable adsorbent in the oil spill treatment. *Journal of Cleaner Production, 170*, 339-350.

45. Wu, Z. Y., Li, C., Liang, H. W., Zhang, Y. N., Wang, X., Chen, J. F., & Yu, S. H. (2014). Carbon nanofiber aerogels for emergent cleanup of oil spillage and chemical leakage under harsh conditions. *Scientific reports*, *4*, 4079. doi.org/10.1038/srep04079.

46. Arfaoui, Dolez, P.I., Dube, M., & David, E. (2017). Development and characterization of a hydrophobic treatment for jute fibres based on zinc oxide nanoparticles and a fatty acid. *Applied Surface Science, 397*, 19-29.

47. Salisu, Z.M., Ishiaku, S.U., Abdullahi, D., Yakubu, M.K., & Diya'uddeen, B.H. (2019). Development of kenaf shive bio–mop via surface deposit technique for water remediation from crude oil spill contamination. *Results in Engineering*.

48. Liu, J., & Wang, X. (2019). A new method to prepare oil adsorbent utilizing waste paper and its application for oil spill clean-ups. *BioResources*.

49. Wang, J., Zheng, Y., & Wang, A. (2012). Superhydrophobic kapok fiber oil-absorbent: Preparation and high oil absorbency. *Chemical Engineering Journal, 213*, 1-7.

50. Korhonen, J. T., Kettunen, M., Ras, R. H., & Ikkala, O. (2011). Hydrophobic nanocellulose aerogels as floating, sustainable, reusable, and recyclable oil absorbents. *ACS applied materials & interfaces*, *3*(6), 1813–1816. doi.org/10.1021/am200475b.

51. Vlaev, L.T., Petkov, P.S., Dimitrov, A., & Genieva, S. (2011). Cleanup of water polluted with crude oil or diesel fuel using rice husks ash. *Journal of the Taiwan Institute of Chemical Engineers, 42*, 957-964.

52. Nguyen, S.T., Feng, J., Le, N.T., Le, A.X., Hoang, N.H., Tan, V.B., & Duong, H.M. (2013). Cellulose Aerogel from Paper Waste for Crude Oil Spill Cleaning. *Industrial & Engineering Chemistry Research, 52*, 18386-18391.

53. Coury, C., & Dillner, A.M. (2009). ATR-FTIR characterization of organic functional groups and inorganic ions in ambient aerosols at a rural site. *Atmospheric Environment, 43*, 940-948.

54. Gregg, S. J. Sing, K. S. W. (1982). Adsorption, surface area and porosity, *Academic Press: London*, 1982.

55. Kumagai, S., Noguchi, Y., Kurimoto, Y., & Takeda, K. (2007). Oil adsorbent produced by the carbonization of rice husks. *Waste management (New York, N.Y.)*, *27*(4), 554–561. doi.org/10.1016/j.wasman.2006.04.006.

56. Lowell, S., Shields, J. E., Thomas, M. A., & Thommes, M. (2012). *Characterization of porous solids and powders: surface area, pore size and density* (Vol. 16). Springer Science & Business Media.

57. Lim, T. T., & Huang, X. (2007). Evaluation of kapok (Ceiba pentandra (L.) Gaertn.) as a natural hollow hydrophobic-oleophilic fibrous sorbent for oil spill cleanup. *Chemosphere*, *66*(5), 955–963. doi.org/10.1016/j.chemosphere.2006.05.062.

58. Ahmad, A.L., Chan, C.Y., Shukor, S.R., & Mashitah, M.D. (2009). Adsorption kinetics and thermodynamics of β-carotene on silica-based adsorbent. *Chemical Engineering Journal, 148*, 378-384.

59. Li, G., Chen, X., & Huang, Y. (2015). Contact Angle Determined by Spontaneous Imbibition in Porous Media: Experiment and Theory. *Journal of Dispersion Science and Technology, 36*, 772 - 777.

60. Yu, B. (2008). Analysis of Flow in Fractal Porous Media. *Applied Mechanics Reviews, 61*, 050801.

61. Liu, Y., Yu, B., Xu, P., & Wu, J. (2007). STUDY OF THE EFFECT OF CAPILLARY PRESSURE ON PERMEABILITY. *Fractals, 15*, 55-62.

62. Cai, J., Yu, B., Zou, M., & Luo, L. (2010). Fractal Characterization of Spontaneous Co-current Imbibition in Porous Media. *Energy & Fuels, 24*, 1860-1867.

63. Johnson, R. F., Manjreker, T. G., & Halligan, J. E. (1973). Removal of oil from water surfaces by sorption on unstructured fibers. *Environmental science & technology*, *7*(5), 439–443. doi.org/10.1021/es60077a003.

64. Saba, N., Jawaid, M., Alothman, O.Y., Inuwa, I., & Hassan, A. (2017). A review on potential development of flame retardant kenaf fibers reinforced polymer composites. *Polymers for Advanced Technologies, 28*, 424-434.

65. Washburn, E.W. (1921). The Dynamics of Capillary Flow. *Physical Review, 17*, 273-283.

66. Sahre, K., Schulze, U., Hoffmann, T., Elrehim, M.A., Eichhorn, K., Pospiech, D., Fischer, D., & Voit, B. (2006). Monitoring of chemical reactions during polymer synthesis by real-time attenuated total reflection (ATR)–FTIR spectroscopy. *Journal of Applied Polymer Science, 101*, 1374-1380.

67. Coury, C., & Dillner, A.M. (2008). A method to quantify organic functional groups and inorganic compounds in ambient aerosols using attenuated total reflectance FTIR

spectroscopy and multivariate chemometric techniques. *Atmospheric Environment, 42*, 5923-5932.

68. Golova, O.P. (1975). Chemical Effects of Heat on Cellulose. *Russian Chemical Reviews, 44*, 687-697.

69. Tremblay, L., Alaoui, G., & Léger, M.N. (2011). Characterization of aquatic particles by direct FTIR analysis of filters and quantification of elemental and molecular compositions. *Environmental science & technology, 45 22*, 9671-9.

70. Rosu, C., Negulescu, I., Cueto, R., Laine, R.A., & Daly, W.H. (2013). Synthesis and Characterization of Complex Mixtures Consisting of Cyclic and Linear Polyamides from Ethyl Bis-Ketal Galactarates. *Journal of Macromolecular Science, Part A, 50*, 940 - 952.

71. https://www.hartenergy.com/ep/exclusives/investing-oil-spill-response-and-containment-30980.